Computational study of lanthanide(III) hydration†

Jan Ciupka, Xiaoyan Cao-Dolg, Jonas Wiebke and Michael Dolg*

Received 20th May 2010, Accepted 23rd July 2010
DOI: 10.1039/c0cp00639d

Lanthanide(III) hydration was studied by utilizing density-functional theory and second-order Møller–Plesset perturbation theory combined with scalar-relativistic 4f-in-core pseudopotentials and valence-only basis sets for the Ln^{III} ions. For $[Ln^{III}(H_2O)_h]^{3+}$ (h = 7, 8, 9) and $[Ln^{III}(H_2O)_{h-1}\cdot H_2O]^{3+}$ (h = 8, 9) molecular structures, binding energies, entropies and energies of hydration as well as Gibbs free energies of hydration were calculated using (8s7p6d3f2g)/[6s5p5d3f2g] basis sets for Ln^{III} and aug-cc-pV(D,T)Z basis sets for O and H in combination with the COSMO solvation model. At the generalized gradient approximation level of density-functional theory a preferred hydration number of 8 is found for La^{III}–Tm^{III} and 7 for Yb^{III}–Lu^{III}, whereas hybrid density-functional theory predicts a hydration number 8 for all Ln^{III}. At the SCS-MP2 level of theory the preferred hydration number is found to be 9 for La^{III}–Sm^{III} and 8 for Eu^{III}–Lu^{III} in good agreement with experimental evidence.

1. Introduction

Since the civil use of nuclear power generation is accompanied by problems regarding the disposal of nuclear waste[1] and recycling of spent nuclear fuel[2] the aqueous chemistry of lanthanide as well as actinide ions, especially in lanthanide–actinide and actinide–actinide separation processes, has received special interest.[3] This is due to the fact that modern separation methods rely on two-phase solvent extraction and ion exchange often involving an aqueous phase.[4] Current used nuclear fuel work-up starts with the PUREX[3] process to separate out uranium and plutonium. The remaining highly radiotoxic liquid waste contains long lasting radioactive minor actinides Np, Am and Cm that prohibit economical and ecological long term storage.[5] In order to reduce the radiotoxicity of the liquid waste in the future, neutron irradiation poses an alternative to transmute the minor actinides into nuclides with shorter radioactive half-life. At this step of processing the separation of lanthanides and actinides is indispensable since lanthanides (Gd, Eu and Sm) have high neutron capture cross sections and therefore more likely absorb the neutrons[6] than the actinides. Understanding the hydration of lanthanides as well as of actinides in terms of calculating relative stabilities, complexation constants and selectivity factors[5,7,8] is therefore crucial to the development of new ligands in future extraction processes.

As there are numerous experimental and theoretical studies on the lanthanide hydration only a brief overview can be given here. Since the thermodynamically most stable oxidation state of the lanthanides in aqueous solution is $+III$[9] almost all work in this field is concerned with this oxidation state. The hydration of Ln^{III} has been mainly investigated by neutron diffraction (ND),[10–15] X-ray diffraction (XD)[16–21] and extend X-ray absorption spectroscopy (EXAFS).[22–24] Reported hydration numbers are 9 for La^{III}–Pm^{III} and 8 for Tb^{III}–Lu^{III}, whereas for Sm^{III}–Gd^{III} non-integral hydration numbers indicate a gradual change from 9 to 8. Average Ln^{III}–O distances vary within ±3 pm depending on Ln^{III}, counterion and method of determination; yet the general trend of decrease in Ln^{III}–O distances from La^{III} to Lu^{III}, *i.e.* the lanthanide contraction is reasonably well reproduced.

When the Ln^{III} hydration is treated computationally, problems arise due to the large number of electrons involved (I), the importance of relativistic effects (II) and the open f-shell (III) of the lanthanides. Most investigations use pseudopotentials (PPs) in combination with density-functional theory (DFT) to somewhat overcome (I) and (II) and, in case of use of f-in-core pseudopotentials, also (III). The majority of theoretical investigations is concerned with thermodynamic features and the molecular structures of $[Ln^{III}(H_2O)_h]^{3+}$ (h = 8, 9) for selected lanthanides like Ce,[25] La,[26] Lu,[26,27] Gd,[28] Nd[29] and Yb.[29] Ln^{III}–O distances are in some cases calculated too long probably due to the neglect of bulk solvation effects.[30] Electronic structure investigations of preferred hydration number are only available for Nd[29] and Yb.[29] Calculated values for ΔG°_{H} can deviate from experimental results up to 100 kJ mol^{-1} depending on the scheme of calculation and the choice of reference experimental data.

To our knowledge there is no computational study for all trivalent lanthanide ions in solution that addresses molecular structure, preferred hydration numbers, thermodynamic properties and Gibbs free energies of hydration. Such results have recently been published by some of the present authors for the actinides.[30] We therefore report the first systematic quantum chemical study of Ln^{III} in solution by first principles that is concerned with all the before mentioned points. Our approach is to model poly-aqua lanthanides $[Ln^{III}(H_2O)_h]^{3+}$ for h = 7, 8, 9 to address questions regarding molecular structure and binding energies. To account for the influence of higher hydration shells, the polarizable continuum model

Institute for Theoretical Chemistry, Universität zu Köln, Greinstr. 4, D-50939 Cologne, Germany. E-mail: m.dolg@uni-koeln.de

† Electronic supplementary information (ESI) available: DFT-BP86, DFT-B3LYP and SCS-MP2 molecular structures, binding energies, entropies and energies of hydration and Gibbs free energies of hydration for $[Ln^{III}(H_2O)_h]^{3+}$ (h = 7, 8, 9) and $[Ln^{III}(H_2O)_{h-1}\cdot H_2O]^{3+}$ (h = 8, 9). See DOI: 10.1039/c0cp00639d

COSMO[31,32] was used to calculate Gibbs free energies of hydration and preferred numbers of water molecules in the first hydration shell. In combination with the Ln^{III} ions we used scalar-relativistic 4f-in-core pseudopotentials[33] together with DFT and perturbation theory methods. In the concept of f-in-core PPs for Ln^{III}, all electrons with a principal quantum number smaller than 5 are included in the PP core and are not treated explicitly. This results in effective 8-electron system with the occupation $5s^25p^65d^06s^0$ for Ln^{III}. Besides the greatly reduced computational cost the problem of capturing static correlation[34] is circumvented since the open f-shell is contained in the PP. Since accurate *ab initio* methods that treat static and dynamic correlation in combination with geometry optimizations are not feasible for systems like $[Ln^{III}(H_2O)_h]^{3+}$ with up to nine water molecules due to the high computational effort the use of large-core PPs together with the formal single-reference DFT approach seems reasonable, as it has been demonstrated before.[35,36]

2. Computational details

Our computational approach to describe Ln^{III} hydration is based on the thermodynamic cycle (*cf.* Fig. 1) proposed by Bryantsev, Diallo and Goddard.[37] The procedure is as follows: Firstly, geometry optimizations of $[Ln^{III}(H_2O)_h]^{3+}$ for $h = 7$, 8, 9, of $[Ln^{III}(H_2O)_{h-1}\cdot H_2O]^{3+}$ for $h = 8$, 9 and of $(H_2O)_h$ for $h = 7$, 8, 9 (initial structures taken from the work Sadlej *et al.*[38]) were carried out in the gas phase. Based on the resulting molecular structures the gas phase binding energies D_0 including zero point energy (ZPE) correction were calculated. In order to determine the hydration energies ΔE_H and Gibbs free energies of hydration the influence of higher hydrations shells upon hydration was approximated by single-point energy calculations of the above mentioned species with their fixed gas phase molecular structure within the COSMO-SCRF (self-consistent reaction field). The hydration energy can be viewed as the ZPE-corrected electronic energy necessary to move Ln^{III} from a fixed position in gas phase to a fixed position in liquid phase. Then,

$$\begin{aligned}\Delta E_H &= -D_0 + \Delta E_{SCRF} \\ &= -D_0 + E_{SCRF}([Ln^{III}(H_2O)_h]^{3+}) - E_{SCRF}((H_2O)_h) \quad (1)\end{aligned}$$

where E_{SCRF} is the difference between the energy within the COSMO-SCRF and the gas phase energy. When considering the Gibbs free energy of hydration not only electronic but also thermodynamic contributions like entropies and enthalpies need to be considered. Therefore the Gibbs free energy of hydration can be written as

$$\begin{aligned}\Delta G^\circ_H &= \Delta H^\circ_H - T\Delta S^\circ_H \\ &\approx H^\circ_{[Ln(H_2O)_h]^{3+}(aq)} - H^\circ_{Ln^{3+}(g)} - H^\circ_{(H_2O)_h(aq)} - T\Delta S^\circ_H \quad (2)\end{aligned}$$

where ΔS°_H denotes the hydration entropy, thus the change in absolute entropy of all involved species when transferring Ln^{III} from gas to liquid phase. ΔH° denote the absolute enthalpies that constitute of electronic, translational, rotational and vibrational contributions. As pointed out by Goddard *et al.*[37] when applying the proposed thermodynamic cycle (*cf.* Fig. 1) it is necessary to include correction terms that arise from different standard states in gas and liquid phase. Therefore the correction terms $\Delta G^{0\to\circ}$ in the upper part of the thermodynamic cycle accounts for the Gibbs free energy of change of 1 mol ideal gas from 1 atm (24.46 L mol^{-1}) to 1 M (1 Mol L^{-1}) at 298.15 K:[37,39]

$$\Delta G^{0\to\circ} = -T\Delta S^{0\to\circ} = RT\ln\left(\frac{V_0}{V^\circ}\right) = RT\ln(24.46) \quad (3)$$

The second correction term $\Delta G^{l\to\circ}_{(H_2O)_h}$ account for the Gibbs free energy of change of 1 mol of $(H_2O)_h$ gas from $55.34/h$ M liquid state to 1 M (at 298.15 K):[37]

$$\Delta G^{l\to\circ}_{(H_2O)_h} = -RT\ln\left(\frac{55.34}{h}\right) \quad (4)$$

In order to make a quantitative statement about the preferred hydration number of Ln^{III} the transfer

$$[Ln(H_2O)_h\cdot H_2O]^{3+}(aq) \xrightarrow{trans.} [Ln(H_2O)_{h+1}]^{3+}(aq) \quad (5)$$

was considered. In the case of a negative Gibbs free energy of addition ΔE_{trans} for eqn (5), the higher hydration number $h + 1$ is preferred over h and *vice versa* for positive values of ΔE_{trans}.

All calculations at the DFT level of theory were performed with the TURBOMOLE v. 5.10 program package.[40] At the MP2 level of theory the geometry optimization were also carried out with TURBOMOLE while single point energy calculations with larger basis sets were done with the MOLPRO 2006.1 program package.[41] For Ln^{III} the scalar-relativistic energy-consistent 4f-in-core PPs[33] in combination with the Ln^{III} valence-only (6s6p5d)/[4s4p4d] GTO basis sets[42] with additional 2, 1 and 1 diffuse s, p, and d functions, and 3 f and 2 g polarization functions, *i.e.* (8s7p6d3f2g)/[6s5p5d3f2g] basis sets, were used. For all calculations at the DFT level the aug-cc-pVDZ basis set[43,44] was chosen for H and O since it proved to be sufficiently accurate[30,45] for a description of $[Ln^{III}(H_2O)_h]^{3+}$, $[Ln^{III}(H_2O)_{h-1}\cdot H_2O]^{3+}$ and $(H_2O)_h$. Previous investigations indicate that diffuse basis functions at H and O are generally more important than polarization functions with larger angular momentum so that the use of aug-cc-pVDZ basis sets delivers results that are very similar to results achieved with cc-pVQZ basis sets regarding Ln^{III}–O distances, binding energies and basis set superposition error (BSSE).[45] Test calculations on $[Ln^{III}(H_2O)]^{3+}$ showed that the BSSE is

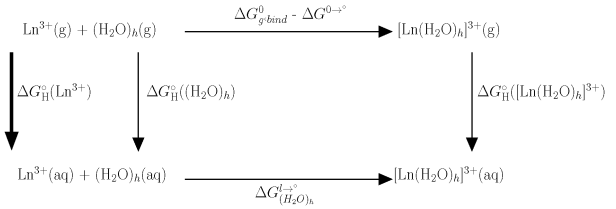

Fig. 1 Underlying thermodynamic cycle for the treatment of the Ln^{III} hydration.

below 0.05 eV when the aug-cc-pVDZ basis set is used. In contrast to that the BSSE exceeds 0.35 eV when a similar basis set without diffuse functions is used. At the MP2 level of theory the aug-cc-pVDZ basis sets for H and O were used for geometry optimizations whereupon single-point energy SCS-MP2[46] calculations with the aug-cc-pVTZ basis sets followed.

For DFT, the GGA functional BP86[47–51] and the hybrid functional B3LYP[47,48,50–53] were used since the former is expected to yield good unscaled vibrational frequencies[54] at advantageous computational costs, and the latter being one of the most successful hybrid functionals incorporating pure HF exchange. For a wavefunction-based perturbational treatment of the Ln^{III} hydration the SCS-MP2 by Grimme[46] as implemented in MOLPRO was used for single-point energy calculations only where the 1s electrons of O were not correlated. For the quadrature of DFT exchange–correlation terms the m4 grid implemented in TURBOMOLE was taken as default for all calculations.[55] SCF thresholds were fixed to 10^{-7} Hartree for the energy and 10^{-4} a.u. for the maximum norm of Cartesian gradient. Geometry optimizations were carried out without symmetry constraints, *i.e.* point group symmetry was set to C_1. True minima on the potential energy surface (PES) were validated by analytical frequency analysis using TURBOMOLEs AOFORCE module. All obtained vibrational frequencies were left unscaled. Regarding nuclides masses[56] only the isotopes with the highest natural abundance[57] were taken into consideration (except Promethium for which the isotope ^{147}Pm was considered). The gas phase entropies of Ln^{III} needed in the calculation of ΔG°_{H} were taken from the work of Bratsch and Lagowski[58] (*cf.* Table 1) who used a modified Sackur-Tedtrode equation that includes a term for the additional electronic entropy caused by the degeneracy of the eletronic state[59] of each lanthanide ion.

Thermodynamic contributions of the molecular structure through vibration and rotation as well as absolute entropies were calculated using the module FREEH contained in the TURBOMOLE package assuming that the treated species form an ideal gas/solution. The temperature and pressure were set to $T = 298.15$ K and $p = 0.1$ MPa, respectively.

Table 1 Reference Ln^{III} Gibbs free energies of hydration ΔG°_{H} (in kJ mol^{-1}), reference calculated hydration numbers h, COSMO PCM cavity radii r_{COSMO} (in pm) and the gas phase entropies for the trivalent cations $S^{\circ}_{gas}(Ln^{3+}$ (in J mol^{-1} K^{-1}))

Ln^{III}	h[60]	ΔG°_{H}[60]	r_{COSMO}	$S^{\circ}_{gas}(Ln^{3+})$[58]
La	9.00	3060.7	203.92	170.28
Ce	9.00	3112.4	200.53	185.28
Pr	9.00	3155.6	197.79	188.72
Nd	9.00	3183.0	196.08	189.89
Pm	8.99	3210.4	194.41	189.10
Sm	8.94	3228.3	193.33	186.54
Eu	8.71	3278.8	190.35	181.18
Gd	8.27	3291.7	189.61	189.11
Tb	8.05	3331.0	187.37	193.28
Dy	8.01	3336.5	187.07	195.29
Ho	8.00	3381.7	184.57	195.98
Er	8.00	3404.1	183.35	196.65
Tm	8.00	3431.4	181.89	194.04
Yb	8.00	3473.3	179.70	190.31
Lu	8.00	3487.7	178.96	173.16

All single-point energy calculations within the COSMO polarizable continuum model (PCM)[31,32] were carried out with permittivity set to infinity while all other parameters were set to their default values. Cavity radii for H and O were set to 130 and 172 pm, respectively, as recommended.[31] Since no recommended values exist for the Ln^{III} ions, these were derived by the following procedure: The Ln^{III} ion was calculated with and without the COSMO PCM at the DFT-BP86 level of theory and the energy difference was used to approximate the Gibbs hydration free energy. Then the COSMO cavity radius r was varied so that the energy difference $E_{gas} - E_{COSMO}$ matched the experimental values for the Gibbs hydration free energy taken from the work of David, Vokhmin and Ionova.[60] The obtained cavity radii for Ln^{III} as well as the reference values for ΔG°_{H} are found in Table 1. This parameterization may seem too simplistic, yet investigations revealed that the choice of r does not influence calculated energies of Ln^{III}–aqua systems within the COSMO PCM as long as r_{COSMO} is not set to an artificially high value so that the cavity sphere of Ln^{III} extends beyond the cavity sphere spanned by the surrounding H and O.[45] Since radii adjusted at the MP2 level of theory deviate less than 1 pm from those obtained with DFT-BP86, the latter were also used for all MP2 calcualtions. For calculations within the COSMO PCM at the SCS-MP2 level of theory the PTE (perturbation theory energy only) approach was chosen since it is the only one formally consistent with second-order perturbation theory.[61,62] In this approach a normal SCS-MP2 calculation is performed on the HF wave function within the COSMO so that the reaction field (response of the solvent) is still at the HF level.

3. Results and discussion

3.1 Ln^{III}–aqua structural aspects

Concerning structural aspects of the primary hydration shell only the most stable structural isomers are considered in the following discussion. For the hydration number $h = 7$ the slightly distorted 1-capped trigonal prism **1** was found to be preferred over the pentagonal bipyramid. This result is also found for the corresponding complexes of the trivalent actinides.[30] For $h = 8$ the preferred structure for all lanthanides is a square antiprism **2** with an approximate point group symmetry S_8. Other conceivable structural isomers like the square prism or the dodecahedron were found to be energetically less stable points on the PES (potential energy surface) with imaginary frequencies. When hydration number $h = 9$ is considered only the 3-capped trigonal prism **3** with point group symmetry D_3 was found as PES-minimum. These findings are in line with other theoretical investigations that find the square antiprism[25,26,28,29] ($h = 8$) and the 3-capped trigonal prism[25,27–29] ($h = 9$) as energetically most stable structures. Since there is no experimental evidence for higher or lower numbers of water molecules in the first hydration shell of the trivalent lanthanide ions, no further investigation on structures of such complexes was performed.

The general observation is that the structural parameters of **1**, **2** and **3** (*cf.* Fig. 2) vary monotonically with the primary hydration number h and the nuclear charge Z such that the

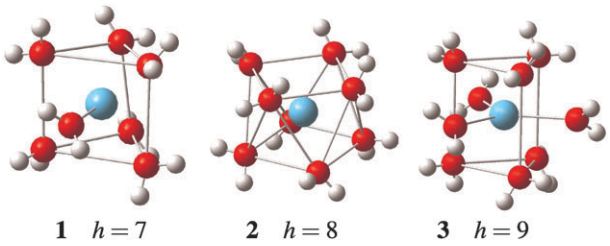

Fig. 2 $[Ln^{III}(H_2O)_h]^{3+}$ calculated gas phase structures. The distorted 1-capped trigonal prism **1**, the square antiprism **2** and the 3-capped trigonal prism **3** have 7, 8 and 9 water molecules in the first hydration shell.

mean Ln^{III}–O distances decrease with increasing Z and decreasing h (*cf.* Table 1, Fig. 3). With increasing Z the mean Ln^{III}–O distance d_{LnO} decreases by 20.9 pm ($h = 7$), 19.9 pm ($h = 8$) and 18.3 pm ($h = 9$) for DFT-BP86 and by 21.1 pm ($h = 7$), 20.2 pm ($h = 8$) and 19.6 pm ($h = 9$) for MP2 levels of theory. When using small core pseudopotentials (SPPs)[63–65] a decrease of 21 pm is obtained at DFT-BP86 for $h = 8$. These values are in line with relativistic studies of the lanthanide contraction[66,67] as well as with relativistic all-electron studies on $[Ln^{III}(H_2O)]^{3+}$ systems.[68]

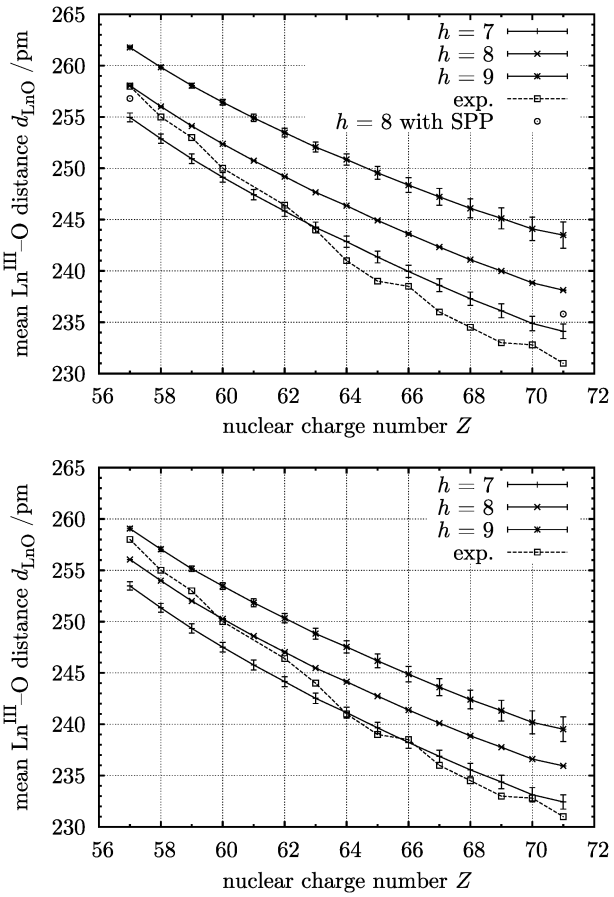

Fig. 3 Mean Ln^{III}–O distances d_{LnO} for $[Ln^{III}(H_2O)_h]^{3+}$ systems at the DFT-BP86 (top) and MP2 (bottom) levels of theory; increasing d_{LnO} error bars are caused by non-symmetry equivalent Ln^{III}–O distances that deviate from the total average value; experimental values from EXAFS and X-ray spectroscopy are taken from the work of David and Fourest.[69]

The bonding situation in these complexes can be described as mostly electrostatic since Mulliken and natural charges of +2.2 to +2.9 and +2.65 to +2.55, respectively, are found for the lanthanide ions. Mulliken charges suggest more ionic bonding towards higher numbers of Z which is observed in form of less charge donations from the water and thus higher effective charges on the lanthanide ions. Since Mulliken charges are known to be of limited validity[70] natural charges based on a natural population analysis (NPA)[71] were also calculated. These support the general idea of a highly electrostatic bonding situation, yet the trend of increasing ionic bonding with increasing Z cannot be confirmed since natural charges for all lanthanide ions remain between +2.65 and +2.55. Therefore only the character of a highly electrostatic bonding but neither the trend of increasing nor decreasing covalent bonding with water ligands along the lanthanides can be confirmed. If covalent bonding is present in $[Ln^{III}(H_2O)_h]^{3+}$ species this is due to participation of the 5d- rather than 4f-orbitals[35] since the less compact 5d-orbitals are vacant in the free trivalent ion and therefore a donation from the H_2O $3a_1$ orbital is possible,[68] however quantitative statements cannot be made based on the obtained data. Yet the fact of a minor role of the f-orbitals in ligand bonding justifies the use of large f-in-core PPs a posteriori. We note here that due to the adjustment of the f projector the 4f-in-core PPs can accept some excess electron density in the 4f-shell, *i.e.* a ligand to Ln 4f charge transfer could occur to some extent.

In comparison with neutron diffraction (ND),[10–15] X-ray diffraction (XD)[16–21] and extend X-ray absorption fine structure spectroscopy (EXAFS)[22–24] data, the calculated Ln^{III}–O distances (*cf.* Table 2, Fig. 3) are systematically overestimated by DFT methods, but the general trend with increasing Z is well reproduced. The overestimation of Ln^{III}–O distances is mainly ascribed to the neglect of bulk solvation that could be addressed by either explicit inclusion of higher hydration shells or by use of a continuum solvation model during the geometry optimization process.[72,73] Both possibilities lead to difficulties which are not straightforward to overcome, *i.e.* the multiple

Table 2 Mean Ln^{III}–O distances d_{LnO} for $[Ln^{III}(H_2O)_h]^{3+}$ at the DFT-BP86 and MP2 levels of theory (in pm)

	DFT-BP86			MP2		
	$h = 7$	$h = 8$	$h = 9$	$h = 7$	$h = 8$	$h = 9$
La	255.0	258.0	261.8	253.5	256.1	259.1
Ce	252.9	256.0	259.8	251.3	254.0	257.1
Pr	250.9	254.1	258.1	249.3	252.0	255.1
Nd	249.1	252.4	256.4	247.5	250.3	253.5
Pm	247.4	250.7	254.9	245.8	248.6	251.8
Sm	245.8	249.2	253.5	244.1	247.0	250.3
Eu	244.2	247.7	252.1	242.5	245.5	248.8
Gd	242.9	246.3	250.8	241.1	244.1	247.5
Tb	241.6	244.9	249.5	239.7	242.7	246.2
Dy	240.0	243.6	248.4	238.2	241.4	244.9
Ho	238.6	242.3	247.2	236.9	240.1	243.6
Er	237.3	241.1	246.1	235.6	238.9	242.4
Tm	236.1	240.0	245.1	234.4	237.8	241.3
Yb	234.9	238.8	244.1	233.1	236.6	240.2
Lu	234.1	238.1	243.5	232.4	235.9	239.5

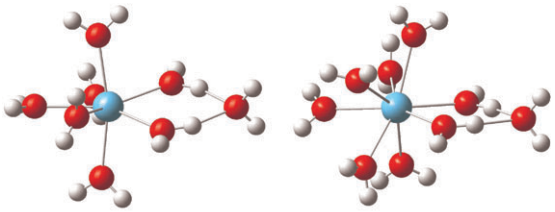

4 $h-1=7$ **5** $h-1=8$

Fig. 4 $[Ln^{III}(H_2O)_{h-1}\cdot H_2O]^{3+}$ calculated gas phase structures with $h-1$ water molecules in the 1st and one water molecule in the 2nd hydration shell.

minima problem and convergency problems, respectively. As an approximation to the higher hydration shells, the systems $[Ln^{III}(H_2O)_{h-1}\cdot H_2O]^{3+}$ (h = 8, 9) with $h-1$ water molecules in the first hydration and 1 water molecule in the second hydration shell were considered. The $[Ln^{III}(H_2O)_{h-1}\cdot H_2O]^{3+}$ complexes were modeled by taking the corresponding $[Ln^{III}(H_2O)_{h-1}]^{3+}$ systems and let an additional water molecule coordinate two water molecules in the first hydration shell in an η^2 fashion. As most stable structures **4** and **5** were found (*cf.* Fig. 4). Depending on the DFT functional and h there is a decrease in the mean Ln^{III}–O distance d_{LnO} of up to 0.7 pm if one water molecule is present in the 2nd hydration shell. This is due to significantly shorter Ln^{III}–O distance for the two water molecules in 1st hydration shell that are coordinated by the one in the 2nd hydration shell. The decrease of d_{LnO} with Z for $[Ln^{III}(H_2O)_{h-1}\cdot H_2O]^{3+}$ at the DFT-BP86 level of theory is 20.7 pm and 19.9 pm for h = 8 and h = 9, respectively.

When going to the MP2 level of theory mean Ln^{III}–O distances d_{LnO} are shorter for $[Ln^{III}(H_2O)_h]^{3+}$ (h = 7, 8, 9) systems than any calculated DFT values (*cf.* Table 2, Fig. 3) so that the overestimation in comparison to experimental results[69] is fairly small. Obviously, the neglect of bulk solvation effects at this level of theory does not lead to significantly different geometric parameters from those experimentally observed. When considering $[Ln^{III}(H_2O)_{h-1}\cdot H_2O]^{3+}$ systems similar to DFT, a decrease in mean d_{LnO} of about 0.5 pm for the 1st hydration shell is observed. This may indicate that an explicit treatment of the 2nd hydration shell is necessary to obtain an accurate structural representation of the solvated lanthanide ions. However we believe that problems of finding and the consideration of several important minima structures to account for dynamic effects in solvation make the explicit modeling of higher hydration shells quite unfavorable in the comparison with only modeling the 1st hydration shell explicitly and using a continuum solvation model. The lower structural complexity in the latter case makes it much easier to find the global minima. Hence the following discussion of binding energies, hydration energies and entropies as well Gibbs free energies of hydrations is addressed to $[Ln^{III}(H_2O)_h]^{3+}$ systems with only the 1st hydration shell treated explicitly. Due to the similarity of the DFT-BP86 and DFT-B3LYP results, the latter are not discussed here explicitly but the corresponding data can be found in the electronic supplementary information (ESI†).

3.2 Ln^{III} binding energies, hydration energies, hydration entropies and Gibbs free energies of hydration

Corresponding to

$$Ln^{3+}(g) + (H_2O)_h(g) \rightarrow [Ln(H_2O)_h]^{3+}(g), \qquad (6)$$

ZPE-corrected gas phase binding energies D_0 of $[Ln^{III}(H_2O)_h]^{3+}$ with respect to water clusters of equivalent size are given in Table 3. The gas phase binding energies D_0 increase with increasing Z due to decreasing ion radii and therefore shorter Ln^{III}–O distances accompanied by stronger electrostatic interactions. D_0 increases also with h because more water molecules are involved in coordination, yet the per-molecule binding energy decreases with increasing h which is attributed to the growing importance of H_2O–H_2O steric interaction and repulsion within the 1st hydration shell. In order to consider hydration energies ΔE_H according to

$$Ln^{3+}(g) + (H_2O)_h(aq) \rightarrow [Ln(H_2O)_h]^{3+}(aq), \qquad (7)$$

D_0 is not a sufficient quantity of description since it neglects bulk phase interactions that were addressed by single-point energy calculations of $[Ln^{III}(H_2O)_h]^{3+}$ and $(H_2O)_h$ within the

Table 3 Negative gas phase binding energies $-D_0$ (first column) according to reaction 6 and difference in ΔE_{SCRF} between $[Ln^{III}(H_2O)_h]^{3+}$ and $(H_2O)_h$ (second column) for DFT-BP86 and SCS-MP2 level of theory (in eV)

	DFT-BP86 $[Ln^{III}(H_2O)_h]^{3+}$						SCS-MP2 $[Ln^{III}(H_2O)_h]^{3+}$					
	h = 7		h = 8		h = 9		h = 7		h = 8		h = 9	
La	−15.97	−15.96	−16.62	−15.55	−17.14	−14.96	−16.08	−16.27	−16.94	−15.65	−17.68	−15.06
Ce	−16.29	−16.17	−16.93	−15.59	−17.45	−15.01	−16.39	−16.29	−17.26	−15.69	−17.98	−15.11
Pr	−16.59	−16.20	−17.23	−15.64	−17.73	−15.06	−16.70	−16.32	−17.56	−15.74	−18.28	−15.16
Nd	−16.87	−16.23	−17.52	−15.68	−18.00	−15.10	−16.98	−16.34	−17.85	−15.78	−18.55	−15.20
Pm	−17.14	−16.26	−17.78	−15.72	−18.25	−15.14	−17.26	−16.37	−18.12	−15.82	−18.80	−15.24
Sm	−17.40	−16.28	−18.03	−15.75	−18.49	−15.18	−15.57	−16.39	−18.38	−15.86	−19.05	−15.28
Eu	−17.66	−16.32	−18.29	−15.79	−18.73	−15.22	−17.79	−16.42	−18.65	−15.89	−19.30	−15.32
Gd	−17.90	−16.34	−18.53	−15.83	−18.95	−15.25	−18.03	−16.44	−18.89	−15.93	−19.52	−15.35
Tb	−18.15	−16.37	−18.77	−15.86	−19.18	−15.29	−18.29	−16.47	−19.14	−15.96	−19.75	−15.39
Dy	−18.39	−16.41	−19.01	−15.90	−19.40	−15.32	−18.54	−16.51	−19.38	−16.00	−19.97	−15.42
Ho	−18.63	−16.43	−19.24	−15.93	−19.61	−15.35	−18.78	−16.53	−19.62	−16.03	−20.19	−15.47
Er	−18.87	−16.46	−19.46	−15.97	−19.82	−15.40	−19.03	−16.56	−19.85	−16.06	−20.40	−15.50
Tm	−19.08	−16.48	−19.67	−16.00	−20.01	−15.43	−19.26	−16.58	−20.08	−16.10	−20.60	−15.53
Yb	−19.31	−16.51	−19.89	−16.03	−20.21	−15.46	−19.48	−16.61	−20.29	−16.13	−20.80	−15.56
Lu	−19.47	−16.54	−20.04	−16.05	−20.35	−15.47	−19.63	−16.63	−20.43	−16.15	−20.93	−15.57

COSMO-SCRF. Then the hydration energy is defined according to eqn (1) with

$$\Delta E_{\mathrm{SCRF}} = E_{\mathrm{SCRF}}([\mathrm{Ln^{III}}(\mathrm{H_2O})_h]^{3+}) - E_{\mathrm{SCRF}}((\mathrm{H_2O})_h) \quad (8)$$

as the difference in COSMO-SCRF stabilization energies given in Table 3. ΔE_{SCRF} increases in magnitude with increasing Z because of decreasing PCM cavity size whereas the opposite trend is observed with increasing h. Quantitatively, the $\mathrm{Ln^{III}}$ hydration energies are very similar and almost the same for $h = 7, 8, 9$ at the DFT-BP86 level of theory. SCS-MP2 ΔE_{SCRF} values are generally more negative than DFT results but $h = 7$ yields slightly less negative hydration energies at the SCS-MP2 level (*cf.* Fig. 5). The similarity in magnitude of different hydration numbers can be explained by a simultaneous increase of D_0 and absolute decrease of ΔE_{SCRF} with increasing h (*cf.* Table 3) so that the sensitive interaction of binding and SCRF stabilization energies determines the hydration number which yields the largest (most negative) hydration energy. In particular, this is $h = 8$ for all lanthanides at the DFT-BP86 level and for the late lanthanides at the SCS-MP2 level. For the early lanthanides at the SCS-MP2 level it is $h = 9$.

Entropies of hydration $\Delta S^{\circ}_{\mathrm{H}}$ needed for Gibbs free energies of hydration where calculated according to

$$\Delta S^{\circ}_{\mathrm{H}} \approx S^{\circ}([\mathrm{Ln^{III}}(\mathrm{H_2O})_h]^{3+}) - S^{\circ}(\mathrm{Ln}^{+\mathrm{III}}) - S^{\circ}((\mathrm{H_2O})_h) \quad (9)$$

where the entropies on the right hand side are absolute entropies of the involved species. For $\mathrm{Ln^{III}}$ the values were taken from work of Bratsch and Lagowski,[58] while the other entropies were calculated with the FREEH module of TURBOMOLE. Calculated hydration entropies (*cf.* Fig. 6) are, as expected, all negative and their trend with increasing Z is identical for all primary hydration numbers and methods used since the gas phase entropies of $\mathrm{Ln^{III}}$ employed in the calculation were all the same tabulated values. Although $\Delta S^{\circ}_{\mathrm{H}}$ values from MP2 calculations are larger in magnitude than these obtained by DFT, all values are generally smaller than available experimental data[74] due to the approximative calculation scheme of hydration entropies using gas phase structures and frequencies.

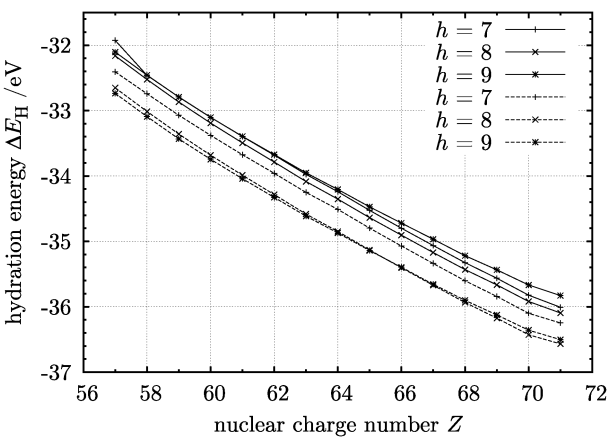

Fig. 5 Hydration energies of $\mathrm{Ln^{III}}$ calculated using eqn (1) for $[\mathrm{Ln^{III}}(\mathrm{H_2O})_h]^{3+}$ and hydration number $h = 7, 8, 9$. Solid lines indicate DFT-BP86 and dashed lines SCS-MP2 results.

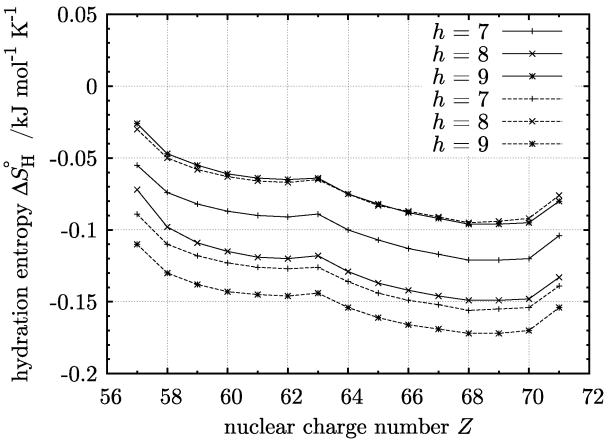

Fig. 6 Hydration entropies of $\mathrm{Ln^{III}}$ calculated using eqn (9) for hydration numbers $h = 7, 8, 9$. Solid lines indicate DFT-BP86 and dashed lines MP2 results.

However they are in comparable range with the experimental values in contrast to the results when h single water molecules instead of a water cluster $(\mathrm{H_2O})_h$ are involved in the thermodynamic cycle (*cf.* Fig. 1) and the entropy calculation according to eqn (9). In the latter calculation scheme the absolute entropy of water molecules in their liquid phase is overestimated since the water molecules were considered independently is assumed which is an approximation to the behavior of an ideal gas and certainly not suitable for descriptions in liquid phase.

Finally, the standard Gibbs free energies of hydration of $\mathrm{Ln^{III}}$ were approximated using eqn (2) and the gas phase molecular structures of $(\mathrm{H_2O})_h$ and $[\mathrm{Ln^{III}}(\mathrm{H_2O})_h]^{3+}$. The absolute enthalpies H° were calculated according to

$$H^{\circ} = E_{\mathrm{elec}} + U_{\mathrm{struc}} + RT, \quad (10)$$

where E_{elec} is the purely electronic energy and U_{struc} the inner energy from vibration and rotation. Since the enthalpy of $\mathrm{Ln^{III}}$(g) is neither available experimentally nor by quantum chemical calculations, it was approximated by $2.5RT + E_{\mathrm{elec}}$ which is the expression for an ideal gas. This approximation may seem unjustified yet the error introduced by it is far below 1% of the calculated standard Gibbs energies of hydration. Since $\Delta G^{\circ}_{\mathrm{H}}$ is dominated by ΔE_{elec}, approximations in $-T\Delta S^{\circ}_{\mathrm{H}}$ and $\Delta U_{\mathrm{struc}}$ should therefore be qualified as less critical. Calculated $\Delta G^{\circ}_{\mathrm{H}}$ values agree well with both sets of experimental values (*cf.* Fig. 7) regarding the behavior with increasing Z and the magnitude of the values. The DFT-BP86 values are closer to the lower end of the spectrum spanned by experimental data whereas the SCS-MP2 results are found very well in between both experimental sets. As expected, $\Delta G^{\circ}_{\mathrm{H}}$ increases in magnitude with increasing Z since D_0 and ΔE_{SCRF} which are the dominant contributors to the Gibbs free energy of hydration increase as well. As SCS-MP2 predicts slightly stronger binding energies, the predicted $\Delta G^{\circ}_{\mathrm{H}}$ is also larger. The hydration number has generally less influence than expected as $\Delta G^{\circ}_{\mathrm{H}}$ is very similar for different h. At the SCS-MP2 level of theory $\Delta G^{\circ}_{\mathrm{H}}$ for $h = 7$ is slightly lower than for $h = 8, 9$. The very smooth decrease in $\Delta G^{\circ}_{\mathrm{H}}$ is attributed to our 4f-in-core PP approach and the inherent average over several electronic states. When treating f electrons explicitly a somewhat less

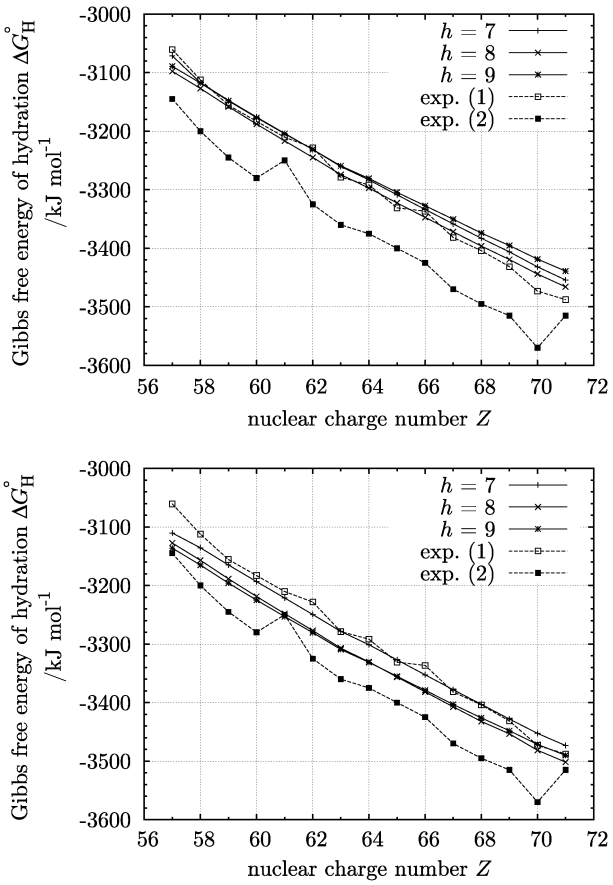

Fig. 7 Ln^{III} Gibbs free energies of hydration calculated according to eqn (2) for primary hydration numbers $h = 7, 8, 9$ at the DFT-BP86 (top) and SCS-MP2 (bottom) level of theory. Experimental results were taken from the work of David, Vokhmin and Ionova (1)[60] and of Marcus (2).[75]

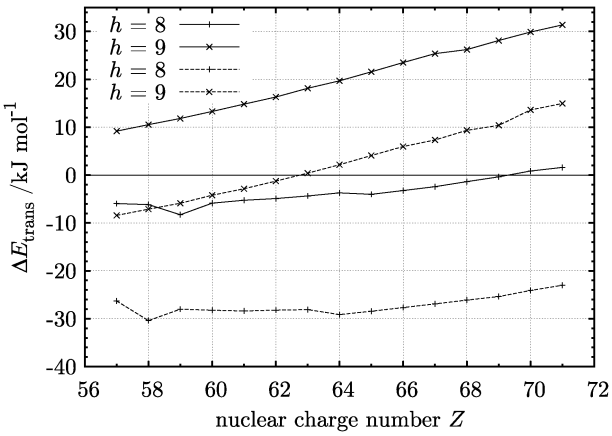

Fig. 8 Reaction energy ΔE_{trans} according to eqn (5) for $h = 8, 9$. Solid lines indicate DFT-BP86 and dashed lines SCS-MP2 results.

smooth behavior with more irregularities is expected. It should be noted however that such irregularities might also be artefacts which arise from a DFT treatment of the open f shells, *e.g.* due to near-degeneracy errors resulting in incorrect splittings of the Ln^{III} state by the ligand field.[76] Calculations using the SPPs[63–65] and the DFT-BP86 yield ΔG°_{H} values of -3120 and -3520 kJ mol^{-1} for lanthanum and lutetium, respectively. These results are also in good agreement with the DFT-BP86 and SCS-MP2 results obtained with the 4f-in-core LPPs (*cf.* Fig. 7).

3.3 Preferred primary hydration numbers

In order to address the question of preferred primary hydration numbers we use a similar approach to that used before in our treatment of the An^{III} hydration[30] based on the addition in eqn (5). The reaction is a hypothetical transfer of a water molecule from the 2nd to the 1st hydration shell and is related to the difference in the chemical potential of $[Ln^{III}(H_2O)_h]^{3+}$ and $[Ln^{III}(H_2O)_{h-1}\cdot H_2O]^{3+}$. The preferred primary hydration number h^* is then defined as the largest h that still yields $\Delta E_{trans} < 0$. ΔE_{trans} increases almost smoothly with Z for $h = 8, 9$ and both quantum chemical methods (*cf.* Fig. 8). This was expected since with increasing Z the Ln^{III}–O distances decrease and the repulsion between water molecules makes higher primary hydration numbers more unfavorable. For DFT-BP86, ΔE_{trans} is negative for all lanthanides except for Yb and Lu for the transfer from $h = 7$ to $h = 8$, whereas the transfer of $h = 8$ to $h = 9$ is always positive indicating that 8 (7 for Yb and Lu) is the preferred primary hydration number. This is not in good agreement with experimental work which predicts a gradual change[69] from $h = 9$ to $h = 8$ between Sm and Tb. In contrast, SCS-MP2 predicts ΔE_{trans} for the transfer from 7 to 8 strongly negative with values between -20 and -30 kJ mol^{-1}. For the transfer from 8 to 9, ΔE_{trans} is calculated decreasingly negative for La to Sm. Starting with Eu the transfer energies become positive indicating the change in preferred primary hydration h^* from 9 to 8 which agrees very well with the mentioned experimental evidence. Regarding the small absolute value of ΔE_{trans} for the two preceding and following elements of Eu, it is assumed that fluctuations between both primary hydration numbers occur.

A more detailed analysis reveals that the inclusion of the influence of higher hydration shells, here accomplished by COSMO PCM, is in fact necessary to predict proper preferred primary hydration numbers. Otherwise without COSMO included, reaction (5) is always positive for the change from $h = 7$ to $h = 8$ or from $h = 8$ to $h = 9$ for DFT level of theory meaning that primary hydration number 7 is preferred over 8 and 9. The reasons for this behavior are generally slightly higher gas phase binding D_0 for $[Ln^{III}(H_2O)_{h-1}\cdot H_2O]^{3+}$ than for $[Ln^{III}(H_2O)_h]^{3+}$ whereas ΔE_{SCRF} is larger (more negative) for the latter one so that in pure gas phase $[Ln^{III}(H_2O)_{h-1}\cdot H_2O]^{3+}$ is always preferred. Regarding the too low predicted primary hydration numbers at the DFT level of theory we assume that repulsion between water molecules is overestimated at that level of theory. Investigations[45] on $[Gd^{III}(H_2O)]^{3+}$ in the extrapolated basis set limit for DFT-BP86, SCS-MP2 and CCSD(T) indicate that pure DFT binding energies without ligand–ligand interaction are even sligthly too large (4.79 eV (DFT-BP86); 4.58 eV (SCS-MP2); 4.63 eV (CCSD(T))) in comparison with other methods which leaves the overestimated water–water repulsion in the primary hydration shell at the DFT level as one possible explanation for underestimated hydration numbers. Other possible explanations are inaccuracies in the DFT description of dispersion

interactions[77] and the overestimated hydrogen bonding strength[78,79] and therefore underestimated hydrogen bond distances which cause too negative ΔE_{SCRF} stabilization energies for the $[Ln^{III}(H_2O)_{h-1}\cdot H_2O]^{3+}$ systems so that they are energetically favoured over the $[Ln^{III}(H_2O)_h]^{3+}$ systems. At the SCS-MP2 level the pure binding energies without ligand–ligand interaction agree well with CCSD(T) results (4.58 eV *vs.* 4.63 eV) and additionally water–water repulsion in the primary hydration sphere does not seem to be overestimated which is reflected by generally shorter Ln–O-distances for $[Ln^{III}(H_2O)_h]^{3+}$ at the MP2 level in comparison with distances calculated at the at the DFT level (*cf.* Fig. 3) This observation is in line with recent results[79] that currently used DFT functionals have to be applied with caution to heavy metal aqua ions even if the problem of capturing static correlation is circumvented by the use of f-in-core PPs.

4. Conclusion

In this work we calculated gas phase molecular structures, binding energies, approximative hydration energies and entropies as well as Gibbs free energies of hydration for $[Ln^{III}(H_2O)_h]^{3+}$ systems with $h = 7, 8, 9$. Our computational approach included the usage of scalar-relativistic Ln^{III} 4f-in-core pseudo-potentials at the DFT and (SCS)-MP2 levels of theory in combination with the COSMO continuum solvation model. At the DFT-BP86 level of theory the results are qualitatively in good agreement with existent experimental[22,60,69,75] and theoretical[25–29] data. Results obtained by (SCS)-MP2 can be considered quantitatively good since both the preferred primary hydration numbers and Gibbs free energies of hydration are predicted in line with experimental data. Mean absolute deviations from both sets[60,75] of experimental data are 36 kJ mol^{-1} (1.1%) and 45 kJ mol^{-1} (1.3%), respectively. Therefore the use of 4f-in-core approximation has not only proven to be applicable to $[Ln^{III}(H_2O)_h]^{3+}$ but also yields results in reasonable agreement with experiment. The same holds for the computational approach to model the first hydration shell explicitly with DFT or SCS-MP2 and to approximate the influence of other hydration shells by use of a continuum solvation model. However our calculations predicted too small primary hydration numbers at the DFT level which is attributed to overestimated hydrogen bonding strengh.

We come to the conclusion that further improvement of the computational approach requires geometry optimizations within the COSMO-SCRF or a similar continuum solvation model that is carefully parameterized and likely non-default. This should yield structures which are in better agreement with experiment than the DFT results presented in this work. To our knowledge optimizations within the COSMO-SCRF are extremely difficult for systems like $[Ln^{III}(H_2O)_h]^{3+}$ due to convergency problems and a significant number of high-order saddle points. Improvement by an explicit treatment of higher hydration shells will require methods like molecular dynamics (MD) simulations to average over the large number of structural configurations which is nearly impossible with a static quantum-chemcial approach. We also belive that the explicit treament of more electrons, *e.g.* the 4f-shell, of the metal will not have a significant impact on the obtained results due to non-participation of the 4f-orbitals in bonding. Moreover the use of DFT methods for the dicussed systems which posses a multi-reference character will introduce more errors, *i.e.* near-degeneracy errors, than the use of the 4f-in-core PPs does. All these points make computational investigations concerning aqueous chemistry of metal ions, which have open electron shells and high coordination numbers, still a challenging task.

References

1 D. C. Hoffman and G. R. Choppin, *J. Chem. Educ.*, 1986, **63**, 1059–1064.
2 *Radiochemistry And Nuclear Chemistry*, ed. G. R. Choppin, J. Liljenzin and J. Rydberg, Butterworth-Heinemann, Woburn, 3rd edn, 2002.
3 G. R. Choppin and K. L. Nash, *Radiochim. Acta*, 1995, **70–71**, 225–236.
4 Z. Kolarik, *Chem. Rev.*, 2008, **108**, 4208–4252.
5 H. H. Dam, D. N. Reinhoudt and W. Verboom, *Chem. Soc. Rev.*, 2007, **36**, 367–377.
6 G. Gryntakis, D. E. Cullen and G. Mundy, *Tech. Rep. Ser. – I. A. E. A.*, 1987, **273**, 199.
7 Y. J. Zhu, J. Chen and R. Z. Jiao, *Solvent Extr. Ion Exch.*, 1996, **14**, 61–68.
8 J. Chen, Y. J. Zhu and R. Z. Jiao, *Sep. Sci. Technol.*, 1996, **31**, 2723–2731.
9 J.-C. G. Bünzli, *Acc. Chem. Res.*, 2006, **39**, 53–61.
10 T. Yamaguchi, *Pure Appl. Chem.*, 1990, **62**, 2251–2258.
11 J. E. Enderby, *Chem. Soc. Rev.*, 1995, **24**, 159–168.
12 R. L. Hahn, *J. Phys. Chem.*, 1988, **92**, 1668–1675.
13 A. H. Narten and R. L. Hahn, *J. Phys. Chem.*, 1983, **87**, 3193–3197.
14 C. Cossy, A. C. Barnes, J. E. Enderby and A. E. Merbach, *J. Chem. Phys.*, 1989, **90**, 3254–3260.
15 B. K. Annis, R. L. Hahn and A. H. Narten, *J. Chem. Phys.*, 1985, **82**, 2086–2091.
16 G. Johansson and H. Wakita, *Inorg. Chem.*, 1985, **24**, 3047–3052.
17 A. Habenschuss and F. H. Spedding, *J. Chem. Phys.*, 1979, **70**, 3758–3763.
18 A. Habenschuss and F. H. Spedding, *J. Chem. Phys.*, 1980, **73**, 442–450.
19 A. Habenschuss and F. H. Spedding, *J. Chem. Phys.*, 1979, **70**, 2797–2806.
20 L. S. Smith and D. L. Wertz, *J. Am. Chem. Soc.*, 1975, **97**, 2365–2368.
21 A. Habenschuss and F. H. Spedding, *J. Chem. Phys.*, 1979, **70**, 3758–3763.
22 I. Persson, P. D'Angelo, S. D. Panfilis, M. Sandström and L. Eriksson, *Chem.–Eur. J.*, 2008, **14**, 3056–3066.
23 M. A. Marques, M. I. Cabaço, M. I. de Barros Marques, A. M. Gaspar and C. M. de Morais, *J. Phys.: Condens. Matter*, 2001, **13**, 4367–4385.
24 T. Yaita, H. Narita, S. Suzuki, S. Tachimori, H. Motohashi and H. Shiwaku, *J. Radioanal. Nucl. Chem.*, 1999, **239**, 371–375.
25 A. Dinescu and A. E. Clark, *J. Phys. Chem. A*, 2008, **112**, 11198–11206.
26 A. E. Clark, *J. Chem. Theory Comput.*, 2008, **4**, 708–718.
27 V. Buzko, I. Sukhno and M. Buzko, *THEOCHEM*, 2009, **894**, 75–79.
28 W. Xiao, Q. Xia, Y. Zhang, L. Ning and Z. Cui, *Chin. J. Chem. Phys.*, 2009, **22**, 395–400.
29 U. Cosentino, A. Villa, D. Pitea, G. Moro and V. Barone, *J. Phys. Chem. B*, 2000, **104**, 8001–8007.
30 J. Wiebke, A. Moritz, X. Cao and M. Dolg, *Phys. Chem. Chem. Phys.*, 2007, **9**, 459–465.
31 A. Klamt, V. Jonas, T. Bürger and J. C. W. Lohrenz, *J. Phys. Chem. A*, 1998, **102**, 5074–5085.
32 A. Klamt and Schüürmann, *J. Chem. Soc., Perkin Trans. 2*, 1993, 799–805.
33 M. Dolg, H. Stoll, A. Savin and H. Preuss, *Theor. Chim. Acta*, 1989, **75**, 173–194.

34 F. P. Rotzinger, *J. Phys. Chem. B*, 2005, **109**, 1510–1527.
35 L. Maron and O. Eisenstein, *J. Phys. Chem. A*, 2000, **104**, 7140–7143.
36 C. P. Groen, Z. Varga, M. Kolontis, K. A. Peterson and M. Hargittai, *Inorg. Chem.*, 2009, **48**, 4143–4153.
37 V. S. Bryantsev, M. S. Diallo and W. A. Goddard III, *J. Phys. Chem. B*, 2008, **112**, 9709–9719.
38 J. Sadlej, V. Buch, J. K. Kazimirski and U. Buck, *J. Phys. Chem. A*, 1999, **103**, 4933–4947.
39 C. P. Kelly, C. J. Cramer and D. G. Truhlar, *J. Chem. Theory Comput.*, 2005, **1**, 1133–152.
40 R. Ahlrichs, M. Bär, M. Häser, H. Horn and C. Kölmel, *Chem. Phys. Lett.*, 1989, **162**, 165–169.
41 R. D. Amos, A. Bernhardsson, A. Berning, P. Celani, D. L. Cooper, M. J. O. Deegan, A. J. Dobbyn, F. Eckert, C. Hampel, G. Hetzer, P. J. Knowles, T. Korona, R. Lindh, A. W. Lloyd, S. J. McNicholas, F. R. Manby, W. Meyer, M. E. Mura, A. Nicklass, P. Palmieri, R. Pitzer, G. Rauhut, M. Schütz, U. Schumann, H. Stoll, A. J. Stone, R. Tarroni, T. Thorsteinsson and H.-J. Werner, *MOLPRO, a package of* ab initio *programs designed by H.-J. Werner and P. J. Knowles, Version 2006.1*, 2006.
42 J. Yang and M. Dolg, *Theor. Chem. Acc.*, 2005, **113**, 212–224.
43 T. H. Dunning, Jr., *J. Chem. Phys.*, 1989, **90**, 1007–1023.
44 R. A. Kendall, R. J. Harrison and T. H. Dunning, Jr., *J. Chem. Phys.*, 1992, **96**, 6796–6806.
45 J. Ciupka, *Diplomarbeit*, Unversität zu Köln, 2010.
46 S. Grimme, *J. Chem. Phys.*, 2003, **118**, 9095–9102.
47 P. A. M. Dirac, *Math. Proc. Cambridge Philos. Soc.*, 1930, **26**, 376–385.
48 A. D. Becke, *Phys. Rev. A: At., Mol., Opt. Phys.*, 1988, **38**, 3098–3100.
49 J. P. Perdew, *Phys. Rev. B: Condens. Matter*, 1986, **33**, 8822–8824.
50 J. C. Slater, *Phys. Rev.*, 1951, **81**, 385–390.
51 S. H. Vosko, L. Wilk and M. Nusair, *Can. J. Phys.*, 1980, **58**, 1200–1211.
52 C. T. Lee, W. T. Yang and R. G. Parr, *Phys. Rev. B: Condens. Matter*, 1988, **37**, 785–789.
53 A. D. Becke, *J. Chem. Phys.*, 1993, **98**, 5648–5652.
54 J. Neugebauer and B. A. Hess, *J. Chem. Phys.*, 2003, **118**, 7215–7225.
55 K. Eichkorn, F. Weigend, O. Treutler and R. Ahlrichs, *Theor. Chem. Acc.*, 1997, **97**, 119–124.
56 M. E. Wieser, *Pure Appl. Chem.*, 2006, **78**, 2051–2066.
57 A. F. Holleman, E. Wiberg, and N. Wiberg, *Lehrbuch der Anorganischen Chemie*, ed. W. de Gruyter, New York, 101st edn, 1995.
58 S. G. Bratsch and J. J. Lagowski, *J. Phys. Chem.*, 1985, **89**, 3310–3316.
59 *Statistical Thermodynamics*, ed. D. A. McQuarrie, Harper & Row, New York, 1st edn, 1973.
60 F. David, V. Vokhmin and G. Ionova, *J. Mol. Liq.*, 2001, **90**, 45–62.
61 F. J. Olivares del Valle and J. Tomasi, *Chem. Phys.*, 1991, **150**, 139–150.
62 J. G. Ángyán, *Int. J. Quantum Chem.*, 1993, **47**, 469–483.
63 X. Cao and M. Dolg, *J. Chem. Phys.*, 2001, **115**, 7348–7355.
64 X. Cao and M. Dolg, *THEOCHEM*, 2002, **581**, 139–147.
65 M. Dolg, H. Stoll and H. Preuss, *J. Chem. Phys.*, 1989, **90**, 1730–1734.
66 W. Küchle, M. Dolg and H. Stoll, *J. Phys. Chem. A*, 1997, **101**, 7128–7133.
67 J. K. Laerdahl, K. J. Faegri, L. Visscher and T. Saue, *J. Chem. Phys.*, 1998, **109**, 10806–10817.
68 Y. Mochizuki and H. Tatewaki, *Chem. Phys.*, 2001, **273**, 135–148.
69 F. H. David and B. Fourest, *New J. Chem.*, 1997, **21**, 167–176.
70 C. Adamo and P. Maldivi, *J. Phys. Chem. A*, 1998, **102**, 6812–6820.
71 A. E. Reed, R. B. Weinstock and F. Weinhold, *J. Chem. Phys.*, 1985, **83**, 735–746.
72 Y. Mochizuki and S. Tsushima, *Chem. Phys. Lett.*, 2003, **372**, 114–120.
73 T. Y. Yang and B. E. Bursten, *Inorg. Chem.*, 2006, **45**, 5291–5301.
74 S. L. Bertha and G. R. Choppin, *Inorg. Chem.*, 1969, **8**, 613–617.
75 Y. Marcus, *J. Chem. Soc., Faraday Trans.*, 1991, **87**, 2995–2999.
76 W. Liu, M. Dolg and L. Li, *J. Chem. Phys.*, 1998, **108**, 2886–2895.
77 P. Wåhlin, C. Danilo, V. Vallet, F. Réal, J.-P. Flament and U. Wahlgren, *J. Chem. Theory Comput.*, 2008, **4**, 569–577.
78 S. Tsushima, *J. Phys. Chem. A*, 2007, **111**, 3613–3617.
79 F. P. Rotzinger, *Chem.–Eur. J.*, 2007, **13**, 800–811.